Green-Synthesis of CuO and Ce-Doped CuO Nanoparticles Using Aqueous Extract of Yam Peel and their Antimicrobial Properties

Article *in* Hybrid Advances · November 2024

DOI: 10.1016/j.hybadv.2024.100335

CITATIONS
4

READS
123

6 authors, including:

Mercy Chisara Ogwuegbu
University of Nigeria
44 PUBLICATIONS **98** CITATIONS
SEE PROFILE

Olatunde Olalekan
Ekiti State University
45 PUBLICATIONS **700** CITATIONS
SEE PROFILE

Trust Pfukwa
University of Johannesburg
17 PUBLICATIONS **158** CITATIONS
SEE PROFILE

Doc Mthiyane
North-West University South Africa Mafikeng
49 PUBLICATIONS **358** CITATIONS
SEE PROFILE

Hybrid Advances 7 (2024) 100335

Contents lists available at ScienceDirect

Hybrid Advances

journal homepage: www.journals.elsevier.com/hybrid-advances

Research Article

Green-synthesis of CuO and Ce-doped CuO nanoparticles using aqueous extract of yam peel and their antimicrobial properties

Mercy C. Ogwuegbu [a,b], Olalekan C. Olatunde [c,d,*], Trust M. Pfukwa [e], Doctor M.N. Mthiyane [a,f], Olaniyi A. Fawole [e], Damian C. Onwudiwe [c,d]

[a] Food Security and Safety Focus Area, Faculty of Natural and Agricultural Science, North-West University (Mafikeng Campus), Private Bag X2046, Mmabatho, South Africa
[b] Department of Animal Science, Faculty of Agriculture, University of Nigeria, Nsukka, 410001, Enugu State, Nigeria
[c] Material Science Innovation and Modelling (MaSIM) Research Focus Area, Faculty of Faculty of Natural and Agricultural Science, North-West University (Mafikeng Campus), Private Bag X2046, Mmabatho, South Africa
[d] Department of Chemistry, School of Physical and Chemical Sciences, Faculty of Natural and Agricultural Science, North-West University (Mafikeng Campus), Private Bag X2046, Mmabatho, South Africa
[e] South African Research Chairs Initiative in Sustainable Preservation and Agroprocessing Research, Postharvest and Agro processing Research Centre, Department of Botany and Plant Biotechnology, University of Johannesburg, P.O. Box 524, Auckland Park, Johannesburg, 2006, South Africa
[f] Department of Animal Science, School of Agricultural Sciences, Faculty of Natural and Agricultural Science, North-West University (Mafikeng Campus), Private Bag X2046, Mmabatho, South Africa

ARTICLE INFO

Keywords:
Drug-resistance
Green synthesis
Antimicrobial
CuO
Ce-doped CuO

ABSTRACT

The rise of drug-resistant microbes presents a critical global health challenge in the 21st century, necessitating the development of potent antimicrobial agents with broad-spectrum activity. Therefore, in this study, we explored the antimicrobial activity of copper oxide (CuO) and cerium-doped CuO (Ce-doped CuO) obtained through a facile green synthesis approach. The nanoparticles were synthesized using aqueous extract of *Dioscorea spp* (yam peel) and characterized for their physicochemical properties using X-ray diffraction (XRD), Fourier-transform infrared spectroscopy (FTIR), electron microscopy, and UV–Vis spectroscopy. Their antimicrobial efficacy was tested against three bacterial strains—*Enterococcus faecalis*, *Escherichia coli*, and *Listeria monocytogenes*—and three fungal strains—*Aspergillus niger*, *Mucor mucedo*, and *Penicillium chrysogenum*. The results demonstrated that cerium doping significantly altered the physicochemical properties of CuO, leading to enhanced antimicrobial activity. The antibacterial zone of inhibition ranged from 7.50 to 16.55 mm for CuO and 11.80–19.50 mm for Ce-doped CuO. For antifungal activity, the minimum inhibitory concentration (MIC) ranged from 0.25 to 0.30 mg/mL for CuO and 0.025–0.03 mg/mL for Ce-doped CuO. Notably, the Ce-doped CuO nanoparticles exhibited antimicrobial effects comparable to standard antibiotics. These findings highlight the potential of green-synthesized Ce-doped CuO nanoparticles as effective antimicrobial agents. By leveraging green synthesis and elemental doping, this study offers a promising solution to combat a wide spectrum of infectious pathogens.

1. Introduction

Antimicrobial agents have been used for over 70 years in the management of infections caused by pathogenic microbes [1]. However, the recent emergence of drug-resistant mutants of these microbes has led to a decrease in effectiveness and withdrawal of some antimicrobial agents from circulation [2]. This has resulted in widespread suffering and is a major global challenge of the twenty-first century [3]. This shows there is a need for novel and improved antimicrobial agents, which have increased research effort into the development and screening of potential antimicrobial agents.

Nanoparticles with antimicrobial activity have emerged as innovative materials due to their capability of generating reactive oxygen species (ROS) such as $O_2^{\bullet-}$, and $^{\bullet}OH$, which can effectively kill pathogens.

* Corresponding author. Material Science Innovation and Modelling (MaSIM) Research Focus Area, Faculty of Faculty of Natural and Agricultural Science, North-West University (Mafikeng Campus), Private Bag X2046, Mmabatho, South Africa.
E-mail address: olalekan.olatunde@eksu.edu.ng (O.C. Olatunde).

https://doi.org/10.1016/j.hybadv.2024.100335
Received 18 September 2024; Received in revised form 29 October 2024; Accepted 20 November 2024
Available online 22 November 2024

In addition, the antimicrobial activity of these materials could also be by enzyme inhibition, metal ion release and membrane disruption [4]. Nanoparticles are increasingly being used as alternatives to antibiotics in different ways including antibiotic delivery systems, antimicrobial coatings in implantable devices, infection prevention, wound healing and microbe detection [5–7]. Several characteristics make nanoparticles suitable alternative to traditional antibiotics such as large-surface-area-to-volume ratio which increases the contact area with target organisms [8]. Furthermore, a complex relationship between the physicochemical properties of nanoparticles such as shape, and the antimicrobial activity of the nanoparticle has been established [9]. This offers a wider room for enhancing the activity of the nanoparticles. Also, a synergistic effect between nanoparticles and traditional antibiotics have been reported [10]. Furthermore, nanoparticles can act on microbes through multiple targets or unique mechanisms, thus making antimicrobial resistance unlikely [11].

Different classes of nanoparticles including metalls, lipid, metal oxides and carbon-based materials have been explored recently as antimicrobial agents. Among these materials metal oxides have gained much attention because of their unique physical and chemical characteristics. The versatility of these materials have also been explored in several applications including drug delivery, sensing, and catalysis. The antimicrobial activity of metal oxides has been ascribed to different properties such as alkalinity, nature of ionic charge and semiconductivity [12–14].

Recently, copper-based nanoparticles such as CuO have gained significant attention in optical sensing, catalysis and therapeutic applications [15,16]. Numerous reports on their antimicrobial activity are also available in literature [17,18]. The interest in these materials is based on their cheaper price and relative abundance in nature, compared to other metals such as gold and silver [19]. Furthermore, the antimicrobial activity of CuO is induced by its generation of oxidative stress and its tendency to alternate between the Cu^{2+} and Cu^{+} oxidation state [19]. This makes CuO a potential material as an antimicrobial agent. Despite its huge antimicrobial potential, CuO nanoparticles suffer from instability when dispersed due to their tendency to aggregate, leading to the formation of large clusters with reduced surface energy [20,21]. This reduces the reactivitiy and antimicrobial efficacy of CuO nanoparticles [21]. To prevent this, CuO nanoparticles are often produced using chemical surfactants such as cetyltrimethylammonium bromide (CTAB) and sodium dodecylbenzene [22,23].

To avoid the use of toxic and expensive surfactants, green synthesis which involves the use of biological components and extracts from plants and organisms such as fungi, algae and bacteria offers a safe and effective route to obtain nanomaterials [24]. Green synthesis offers a synthetic technique with minimized waste generation, environmentally sustainable reaction conditions and the use of nontoxic precursors [25,26]. Interestingly, waste peels from plants such as fruit peels can also be used in the synthesis of nanoparticles [27]. Furthermore, elemental doping reportedly influences nanoparticle morphology alongside, their optical, physical and chemical properties [28]. Also, reports have shown the potential of elemental doping in enhancing the antimicrobial activity of nanoparticles. Cerium ion in particular has been reported to possess unique biological activity due to the tendency to change between the Ce^{3+} and Ce^{4+} oxidation state [29,30]. The dynamic transition between Ce^{3+} and Ce^{4+} is important for maintaining antimicrobial activity. Ce^{4+} initiates ROS production, while Ce^{3+} is reoxidized back to Ce^{4+}. This cycle leads to the continuous generation of ROS and a sustained oxidative stress on microbial cells [31]. Therefore, a Ce-doped CuO nanoparticle synthesized through a green synthesis technique could offer an antimicrobial agent with enhanced antimicrobial activity.

In this study, we report for the first time the green synthesis of CuO and Ce-doped CuO nanoparticles using aqueous extract of waste yam peel. The obtained nanoparticles were characterized for their physicochemical and electronic properties. The antimicrobial efficacy of the nanoparticles was evaluated against three bacterial strains: *Enterococcus faecalis*, *Escherichia coli*, and *Listeria monocytogenes* and three fungi strains: *Aspergillus niger*, *Mucor mucedo*. and *Penicillium chrysogenum*. The study showed the potential of CuO and Ce-doped CuO obtained through a facile green synthesis as an alternative antimicrobial agent for traditional antibiotics.

2. Materials and methods

2.1. Materials

Cerium (IV) sulphate tetrahydrate ($Ce(SO_4)_2•4H_2O$), sodium hydroxide (NaOH), and copper nitrate trihydrate ($Cu(NO_3)_2•3H_2O$) were purchased from Merck, South Africa, while potato dextrose broth (PDB), Muller-Hinton Broth (MHB) and Muller-Hinton Agar (MHA) were purchased from Sisco research laboratories (Mumbai, India). All the chemicals were of analytical grade and were used without further purification.

2.2. Yam peel extract preparation

The yam peel was collected from domestic waste and sun-dried before being ground into powder. Afterwards, 20 g of the yam peel powder was weighed into a 200 mL beaker and 100 mL of distilled water was added. The mixture was stirred at 80 °C for 1 h and was allowed to cool to room temperature. The mixture was filtered, and the obtained aqueous extract was stored in a sealed container at 4 °C for future use.

2.3. Synthesis of CuO and Ce-doped CuO nanoparticles

The method reported by Ogwuegbu et al. [32] with slight modification was used in the synthesis of CuO and Ce-doped CuO nanoparticles. In the synthesis of CuO, 5 g of $Cu(NO_3)_2•3H_2O$ was dissolved in 10 mL of distilled water. Subsequently, 20 mL of the aqueous yam peel extract was added to the mixture. To adjust the pH to 10, 1 M NaOH was drop wisely added to the mixture and the deep blue mixture obtained was stirred vigorously at 80 °C for 2 h. The product was recovered and washed (with a 50:50 vol ratio of water/acetone) by centrifuging the mixture at 5000 rpm for 10 min. The obtained precipitate was dried overnight under vacuum and subsequently calcined for 3 h at 400 °C. For the synthesis of Ce-doped CuO, 0.5 g of $Ce(SO_4)_2•4H_2O$ was added to the $Cu(NO_3)_2•3H_2O$ solution. Afterwards the method described for CuO synthesis followed. The schematic for the synthesis of Ce-doped CuO is shown in Fig. 1.

2.4. Characterization of CuO and Ce-doped CuO nanoparticles

A D8 advance diffractometer (BRUKER AXS, Germany) with Cu Kα radiation (λ = 154.18 p.m.) and operating in Bragg-Brentano mode was used in studying the structural properties of the material. The functional groups present in the materials were investigated through Fourier-transformed infrared spectroscopy (FTIR) carried out on a Spectroquant® 300 spectrophotometer with a wavenumber range of 500–5000 cm^{-1}. Morphological studies were carried out with scanning electron microscopy (SEM) and transmission electron microscopy (TEM) recorded on TECNAI G2 (ACI) equipment (Hillsboro, OR, USA) operating with an accelerating voltage of 200 kV. A spectroquant® Prove 300 spectrophotometer was used for studying the optical properties of the materials. The absorbance of the samples was measured using methanol as solvent within the wavelength range of 200–900 nm.

2.5. Microbial strain preparation

In this study, one Gram-negative (*Eschericiah coli*, ATCC 25922) and two Gram-positive strains (*Enterococcus faecalis*, ATCC 29212 and *Listeria monocytogenes*, ATCC 7644) bacteria strains were used. These strains were kept on Mueller Hinton Agar (MHA) and subculturing was

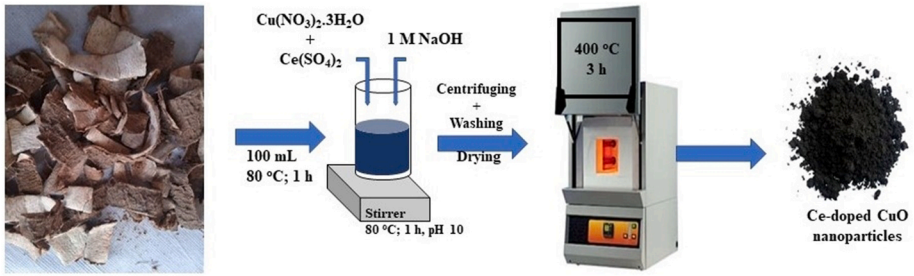

Fig. 1. Schematic for the synthesis of Ce-doped CuO from aqueous extract of yam peel.

also done on the same media at 37 °C. The fungi strains–*Aspergillus niger*, *Mucor mucedo*, and *Penicillium chrysogenum*,–were isolated from decayed strawberry fruit. The fungi showing fast growth were consistently isolated and identified as described by Campbell et al. [33] and López et al. [34]. The fungal pathogens were maintained and subcultured using a Potato Dextrose Agar (PDA) medium at 25 °C.

2.6. Evaluation of antibacterial activity

The agar well diffusion method described by Valgas et al. [35] was used to evaluate the in vitro antibacterial effectiveness of CuO and Ce-doped CuO nanoparticles. Furthermore, the direct suspension method was employed in preparing the inoculum for *Enterococcus faecalis*, *Escherichia coli*, and *Listeria monocytogenes* bacterial strains. Colonies of each bacterium were cultured on a MHA medium, after which the colonies were suspended into Mueller Hinton Broth (MHB). The optical density of the suspended colonies was subsequently adjusted to match that of 0.5 McFarland standard. Afterwards, the final inoculum density of approximately 1.5×10^6 was achieved by preparing 1:100 dilutions of the adjusted suspension in sterile MHB. Each inoculum (100 µL) was then pipetted into a MHA plate in triplicates and spread evenly on the surface with a metal spreader. After drying, 6 mm holes were made on each agar plate with aid of a sterile borer. About 80 µL of each test solution of the nanoparticles (6.4, 3.2, 1.6, and 0.8 mg/mL) was pipetted into the wells and the plates were incubated at 36 ± 1 °C under aerobic conditions for 24 h. Neomycin (3.2 mg/mL) was used as the positive control, while sterile distilled water acted as the negative control. The zones of inhibition were measured in mm after incubation and the analyses were done in triplicates.

2.7. Evaluation of antifungal activity

The antifungal activity of the nanoparticles was assessed using the broth microdilution technique, following the procedure outlined by Berkow et al. [36] with minor adjustments. To prepare the inoculum for *Aspergillus niger*, *Mucor mucedo*, and *Penicillium chrysogenum* a 5 × 5 mm section of agar was taken from 5-day-old fungal cultures and placed into McCartney bottles containing 15 mL of potato dextrose broth (PDB) with 0.1 % (v/v) Tween 80 for 72 h. After incubation, the cell suspensions were vortexed and adjusted to match the turbidity of a 0.5 McFarland standard, equivalent to 1-5 × 10^6 CFU/mL. A working suspension was prepared by diluting each adjusted inoculum 1:10 in sterile PDB to achieve a final inoculum size of approximately 1-5 × 10 CFU/mL. The CuO and Ce-doped CuO nanoparticles were dissolved in PDB to create stock solutions, and two-fold serial dilutions were prepared in 96-well plates at twice the desired final concentration, with a total volume of 100 µL per well. Each well was inoculated with 100 µL of the prepared fungal suspension. After inoculation, the nanoparticle concentrations ranged from 3.2 to 0.025 mg/mL. Amphotericin B (1.6 mg/mL) served as the positive control, while sterile and growth control wells contained PDB and inoculum, respectively. The plates were sealed with parafilm and incubated at 37 °C for 48 h. Fungal growth was visually inspected after incubation, and the Minimum Inhibitory Concentrations (MIC) were defined as the lowest nanoparticle concentrations that completely inhibited fungal growth, expressed in mg/mL.

3. Results and discussions

3.1. Structural and chemical properties of CuO and Ce-doped CuO nanoparticles

The formation of CuO and Ce-doped CuO and the crystallinity of the obtained nanoparticles were confirmed from the XRD pattern presented in Fig. 2. The CuO pattern showed peaks that were consistent with the

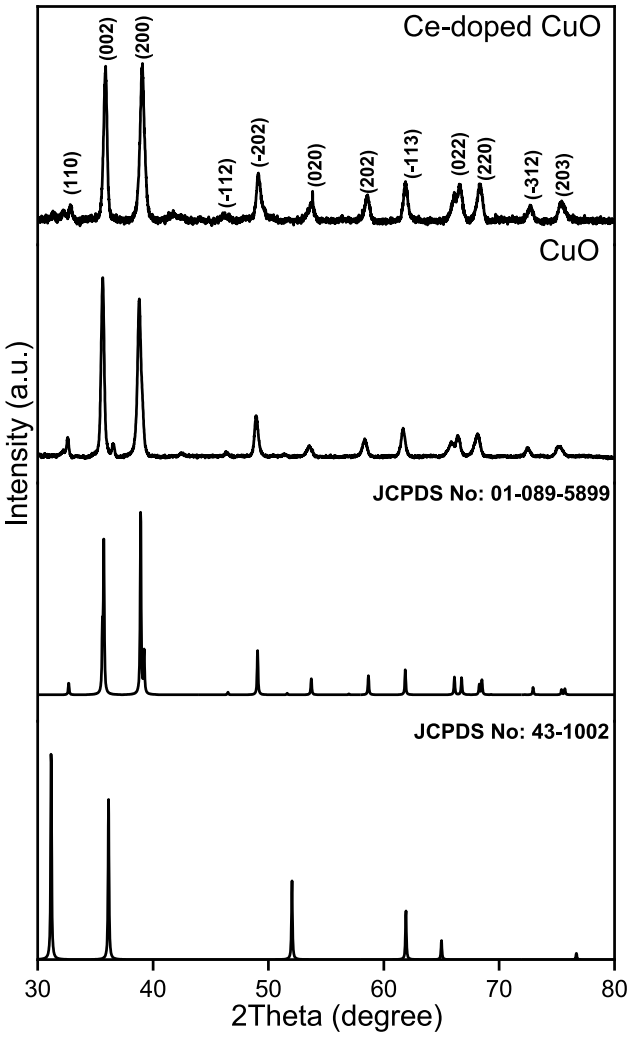

Fig. 2. XRD spectra of CuO and Ce-doped CuO nanoparticles obtained from aqueous extract of yam peel.

monoclinic crystal structure (JCPDS–01–089–5899) [37]. The intensity of the peaks showed highly crystalline CuO nanoparticles were obtained. The XRD pattern of Ce-doped CuO showed a similar pattern to that of CuO, however, the (200) plane was observed to show preferential growth than the (002) plane. This shows the introduction of Ce influenced the direction of growth of the CuO nanoparticle. Furthermore, no addition peaks due to CeO_2 (JCPDS No: 43–1002) was observed in the pattern of Ce-doped CuO, which could be accounted for by the small amount of the dopant.

The crystallite size for the nanoparticles was calculated using the Scherrer equation (Eq. (1)) [38],

$$D = \frac{k\lambda}{\beta \cos\theta} \quad (1)$$

where λ is the wavelength of X-ray, k is a constant (0.94), β is the full width at FWHM of the peak and θ is the diffraction angle. The estimated crystallite size for CuO and Ce-doped CuO is 31.0 and 18 nm respectively. This shows that the introduction of Ce influenced the growth kinetic of the CuO NPs.

Furthermore, to explore the effect of Ce-doping on the structural property of CuO, the lattice strain (ε) inherent in the crystal of the nanoparticles was estimated using Eq. (2).

$$\varepsilon = \frac{\beta}{4\,tan\,\theta} \quad (2)$$

The lattice strain in the crystal of CuO and Ce-doped CuO was estimated to be 3.94×10^{-4} and 7.52×10^{-4}. An increase in the lattice strain was observed with the introduction of Ce, which could be assigned to lattice compression [39]. The dislocation density (ρ_d), a measure of the line defect can also be used to estimate the effect of Ce-doping on the CuO crystal. The dislocation density was calculated using Eq. (3):

$$\rho_d = \frac{1}{D^2} \quad (3)$$

The ρ_d for CuO and Ce-doped CuO was 3.2×10^{-2} and 5.5×10^{-2} line/nm^2. The higher ρ_d aligns with the increased lattice strain in Ce-doped CuO, confirming the alteration in the crystal of CuO induced by doping with Ce.

The lattice parameters of the CuO and Ce-doped CuO nanoparticles (a, b, c and β) were estimated using Eq. (4):

$$\frac{1}{d^2} = \frac{1}{sin^2\,\beta}\left(\frac{h^2}{a^2} + \frac{k^2\,sin^2\,\beta}{b^2} + \frac{l^2}{c^2} - \frac{2hlcos\beta}{ac}\right) \quad (4)$$

where d is the d-spacing and h, k, l are the planes of the CuO structure. The calculated lattice parameters are shown in Table 1. The lattice parameters showed a significant alteration of the crystal structure along the c-plane, arising from Ce-doping.

The FTIR spectrum of the synthesized CuO and Ce-doped CuO are shown in Fig. 3. In the spectra of CuO, the band at 1638 cm^{-1} is ascribed to the O–H group, while the stretching vibrations of the C–H bond was observed at 1061 cm^{-1}. The Cu–O bond was observed at 480 cm^{-1} [40]. In Ce-doped CuO, all the peaks were observed to have shifted into higher wavenumber. This could be ascribed to the introduction of Ce atoms which has different valency, atomic radii and electronic configurations to the host lattice, thus modifying its physical and chemical environment. This results in lattice distortions, strains and variations in bond strength, which influences the vibrational frequencies of the bonds. The overall effect often depends on the dopant's nature, size relative to host ion and its interaction with oxygen atoms in the lattice. The doping of CuO with Ce led to the shortening of the Cu–O bond length, resulting in the shifting of the peaks to higher wavenumbers [41]. In addition, the Ce–O stretching vibration band was observed at 592 cm^{-1} [42]. This confirms the doping of the CuO by Ce.

Table 1
Calculated crystallite size, lattice strain and lattice parameters for CuO and Ce-doped CuO.

	Crystalline size	Lattice strain	a (Å)	b (Å)	c (Å)	β
CuO	31.0	3.94×10^{-4}	4.61	2.70	3.97	127.8
Ce-doped CuO	18.1	7.52×10^{-4}	4.61	2.69	5.00	128.3

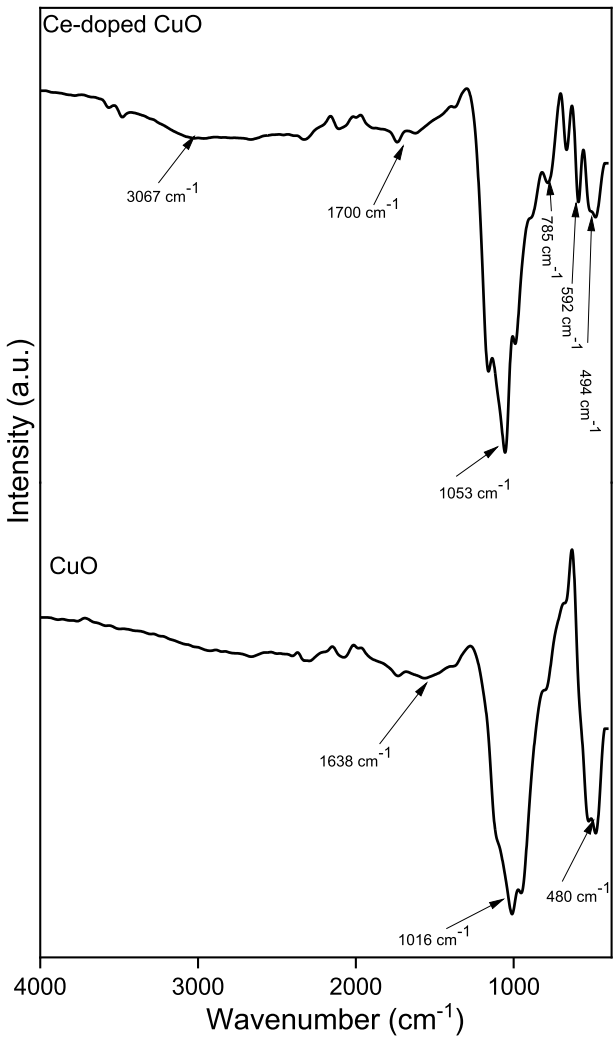

Fig. 3. FTIR spectra of CuO and Ce-doped CuO obtained from the aqueous extract of yam peel.

3.2. Morphological properties of CuO and Ce-doped CuO nanoparticles

The SEM and TEM images of CuO and Ce-doped CuO are shown in Fig. 4. The CuO particles appeared as agglomerated particles with a relatively smooth surface. The granularity of the surface suggests the presence of smaller particles on the surface of large crystallites. The Ce-doped CuO showed significantly altered morphology with the particles appearing more distinct with less agglomeration compared to CuO. The surface appears rougher compared to CuO and the presence of more isolated particles was observed. This shows the presence of Ce influenced the nucleation and growth process of the nanoparticle. The TEM image of CuO shows densely packed clusters of particles. The aggregation of the nanoparticles into large, irregular mass makes the size and shape of the nanoparticle difficult to discern. However, in Ce-doped CuO, the particles show dispersed distribution and are less dense, with more clearly defined individual particles. In addition, the particles

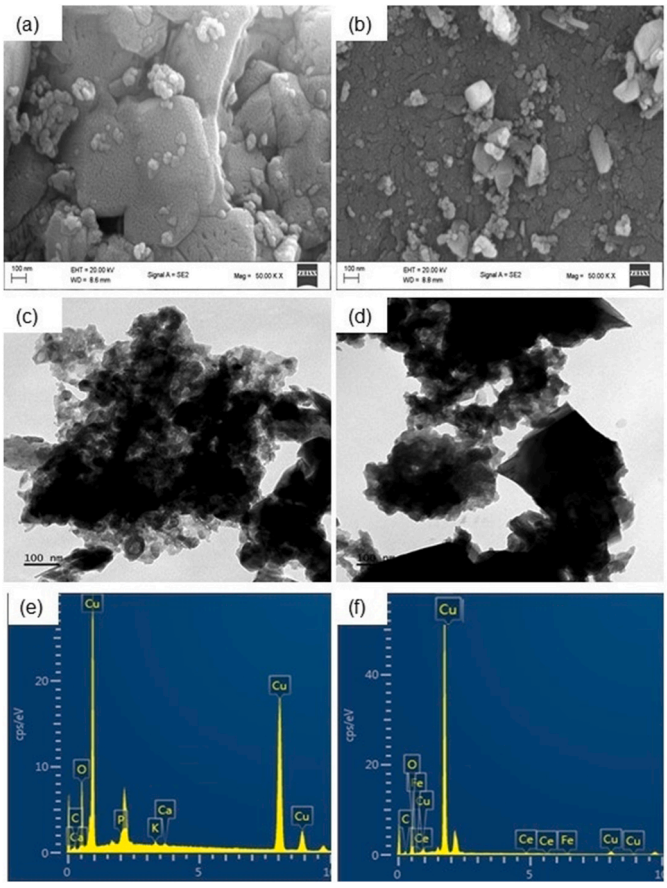

Fig. 4. SEM images of (a) CuO, and (b) Ce-doped CuO; TEM images of (c) CuO, and (d) Ce-doped CuO and EDX spectra of (e) CuO, and (f) Ce-doped CuO.

appear more uniform compared to CuO, signifying a more controlled growth arising from Ce doping. The EDS spectra of CuO, show the presence of Cu and O, which confirms the presence of CuO. The other elements such as Fe, N, are from the plant extracts. The Ce-doped CuO showed the presence of Ce, confirming the doping of the CuO nanoparticle.

3.3. Optical property of CuO and Ce-doped CuO nanoparticles

The optical property of the CuO and Ce-doped CuO nanoparticles was studied through the UV–Vis spectroscopy. Fig. 5a shows the absorption spectra for both CuO and Ce-doped CuO across the UV–Vis spectrum. CuO nanoparticles absorbs mostly in the UV region, around 200–400 nm, beyond which the absorption decreased, showing limited visible light absorption. For Ce-doped CuO, a shift in the absorption edge towards longer wavelengths compared to CuO was observed. In addition, absorption in the UV and visible region was enhanced, implying that Ce-doping enhanced the optical activity in the visible region. This shows the alteration of the electronic structure of CuO by Ce-doping, with a resultant improvement in the utilization of the visible light spectrum. The optical band gap (E_g) of the CuO and Ce-doped CuO were estimated using the Tauc plot as shown in Fig. 5b. The estimated band gap for CuO and Ce-doped CuO was 2.65 eV and 2.41 eV, respectively. The doping of Ce, therefore led to a reduction in band gap allowing it to absorb visible light radiation.

3.4. Antimicrobial study

3.4.1. Antibacterial activity of CuO and Ce-doped CuO nanoparticles

Antibacterial activity of CuO and Ce-doped CuO nanoparticles were analysed against three bacterial strains *Enterococcus faecalis*, *Esherichia coli*, and *Listeria monocytogenes*. Table 2 and Fig. 6 shows the antibacterial activity of CuO and Ce-doped CuO against the bacterial strains in a well-diffusion assay. The result showed that CuO and Ce-doped CuO

Table 2
Effect of concentration of CuO and Ce-doped CuO nanoparticles on zone of inhibition of the growth of some pathogenic bacteria.

	Enterococcus faecalis	Escherichia coli	Listeria monocytogenes
CuO-NPs			
6.4 mg/mL	16.00 ± 0.21^{b}	16.55 ± 0.12^{b}	15.85 ± 0.15^{b}
3.2 mg/mL	13.05 ± 0.41^{c}	12.93 ± 0.61^{c}	13.50 ± 0.38^{c}
1.6 mg/mL	10.17 ± 0.35^{d}	11.23 ± 0.13^{d}	11.20 ± 0.17^{c}
0.8 mg/mL	8.00 ± 0.09^{e}	7.50 ± 0.27^{e}	9.50 ± 0.16^{d}
Neomycin (3.2 mg/mL)	20.00 ± 0.13^{a}	20.00 ± 0.51^{a}	20.50 ± 0.53^{a}
CuO–Ce-NPs			
6.4 mg/mL	19.00 ± 0.36^{ab}	19.50 ± 0.69^{b}	19.00 ± 0.69^{ab}
3.2 mg/mL	16.75 ± 0.57^{b}	16.50 ± 0.53^{c}	16.55 ± 0.64^{b}
1.6 mg/mL	14.50 ± 0.74^{b}	13.60 ± 0.65^{c}	19.20 ± 1.03^{ab}
0.8 mg/mL	12.00 ± 0.56^{c}	12.05 ± 0.43^{d}	11.80 ± 0.06^{c}
Neomycin (3.2 mg/mL)	21.00 ± 0.63^{a}	23.00 ± 0.32^{a}	21.50 ± 1.14^{a}

[a,b,c,d,e] Colums means with different superscripts for each organism between the different concentrations are significantly ($P < 0.05$) different (n = 3).

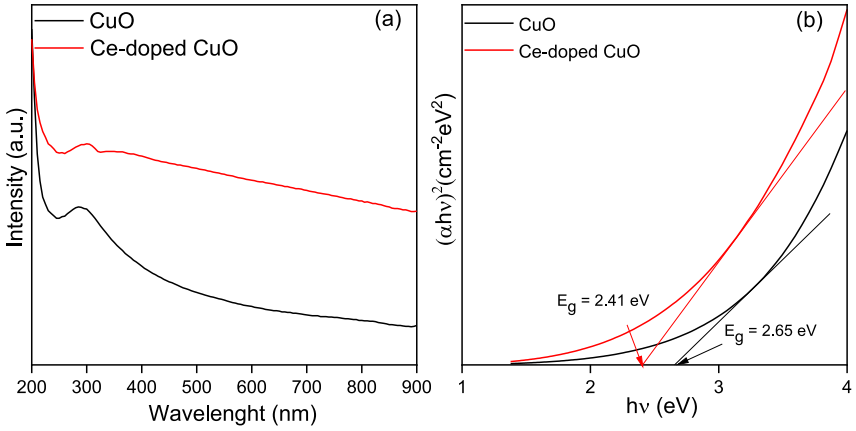

Fig. 5. (a) UV–Vis spectra of CuO and Ce-doped CuO nanoparticles and (b) Tauc plots of CuO and Ce-doped CuO nanoparticles.

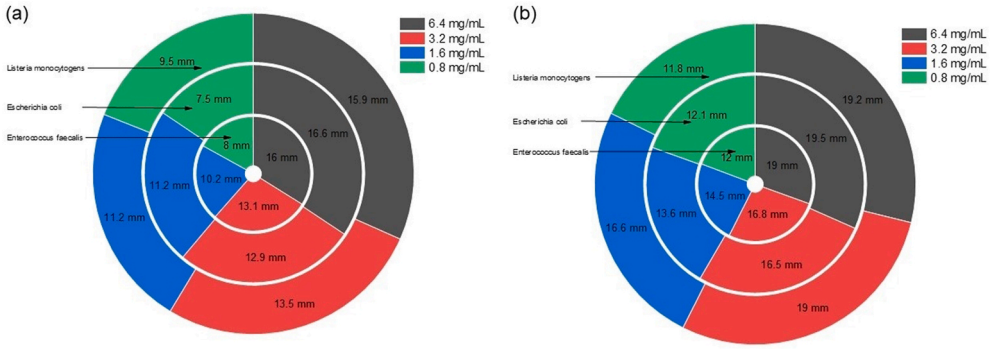

Fig. 6. Multilevel pie chart showing the zone of inhibition of (a) CuO and (b) Ce-doped CuO against *Enterococcus faecalis, Escherichia coli*, and *Listeria monocytogenes*.

demonstrated excellent antimicrobial activity against all three bacterial strains. CuO nanoparticles showed a concentration-dependent activity, with the highest activity observed at 6.4 mg/mL of the nanoparticle. It was also observed that the highest activity of the nanoparticles was against *E. coli* compared to the other bacterial strains. The CuO nanoparticles also exhibited an inhibition zone comparable to the Neomycin standard, showing its potential application for exploration as an antibacterial agent. For Ce-doped CuO nanoparticles the antibacterial activity was observed to be improved relative to CuO. The inhibition zone of CuO nanoparticles ranged from 7.50 to 16.55 mm, whereas for Ce-doped CuO nanoparticles, it ranged from 11.80 to 19.50 mm. Antibacterial activity of nanoparticles has been reported to be significantly influenced by the particle size [43]. Reduced particle size has been reported to enhance the antibacterial activity of nanoparticle [44]. Therefore, the improved activity of Ce-doped CuO nanoparticles could be attributed to its reduced crystallite size compared to CuO. Furthermore, doped nanoparticles have been reported to possess improved ROS generation, which plays an important role in antibacterial activity [45].

Table 3 shows the antibacterial activity of CuO nanoparticles reported in literature compared to this study against *E. Coli*. The Ce-doped CuO compared favourably with other CuO nanoparticles showing their potential antimicrobial activity.

3.4.2. *Antifungal activity of CuO and Ce-doped CuO nanoparticles*

The antifungal activity of CuO and Ce-doped CuO were evaluated against three fungal species – *Aspergillus niger, Mucor mucedo*. and *Penicillium chrysogenum*. The activity of the nanoparticles was compared to the standard antifungal agent, amphotericin. Table 4 and Fig. 7 shows the minimum inhibitory concentration (MIC) of CuO, Ce-doped CuO and amphotericin against the fungal species. The MIC value for CuO ranged from 0.25 to 0.3 (mg/mL), while Ce-doped CuO showed a MIC in the range 0.025–0.03 mg/mL. The highest activity of both CuO and Ce-doped CuO was observed for *Mucor mucedo*, with MIC values of 0.25 mg/mL and 0.025 mg/mL, respectively. The higher activity of Ce-doped CuO compared to CuO could be ascribed to Ce-doping. The Ce-doped

Table 3
Comparison of the antibacterial activity of CuO and Ce-doped CuO with other reported CuO nanoparticles in literature against *E. coli*.

Nanoparticle	Inoculum density	Nanoparticle concentration	Zone of inhibition	Ref
$Cu_{0.96}Ag_{0.02}Zn_{0.02}O$ NPs	10^8 CFU/mL	50 mg/mL	18.5	[46]
CuO NPs	10^8 CFU/mL	25 mg/mL 50 mg/mL	11.3 13.0	[46]
Mg-doped CuO NPs	10^8 CFU/mL	3 mg/mL	22.3	[47]
CuO	10^5 CFU/mL	6.4 mg/mL	16.55	This study
Ce-doped CuO	10^5 CFU/mL	6.4 mg/mL	19.50	This study

Table 4
Minimum Inhibitory Concentration (MIC) of CuO and Ce-doped CuO nanoparticles on the growth of some pathogenic fungi using broth dilution assay.

Organism	MIC value (mg/mL)		
	CuO	Ce-doped CuO	Amphotericin (1.6 mg/mL)
Aspergillus niger	0.3 ± 0.05^a	0.04 ± 0.01^a	0.02 ± 0.01^a
Mucor mucedo	0.25 ± 000^b	0.025 ± 0.01^b	0.025 ± 0.01^a
Penicillium chrysogenum	0.27 ± 0.00^b	0.03 ± 0.00^b	0.025 ± 0.00^a

a,b Row means with different superscripts for each organism between the different concentrations are significantly ($P < 0.05$) different (n = 2).

CuO nanoparticles showed comparative activity to the amphotericin standard, which had a MIC value of 0.025 mg/mL for *Mucor sp*. The size and shape of nanomaterials have been reported to influence their antifungal activity. The large surface-area-to-volume ratio have also been shown to impart enhanced antifungal activity [48]. The lower crystallite size and the alteration in the morphology of Ce-doped CuO could have played a significant role in its improved antifungal activity.

The antifungal activity of CuO and Ce-doped CuO nanoparticles synthesized using aqueous extract of yam peel against *Aspergillus niger* compare favourably with other CuO nanoparticles reported in literature as shown in Table 5.

4. Conclusions

This study presents the facile synthesis of CuO and Ce-doped CuO nanoparticles and the enhanced antimicrobial activity achieved by elemental doping. The improved activity of the doped nanoparticles is ascribed to the modification of the physicochemical property of the nanoparticles, and the tendency of the metal ions to exist in multiple oxidation state. This finding shows that antimicrobial agents with enhanced antimicrobial activity can be obtained through a facile, cost-effective green synthesis route. Furthermore, successful evaluation of the biocompatibility and toxicity of these nanoparticles could make them available for use as alternatives to traditional antimicrobial agents.

CRediT authorship contribution statement

Mercy C. Ogwuegbu: Writing – original draft, Investigation, Data curation, Conceptualization. **Olalekan C. Olatunde:** Writing – original draft, Methodology, Investigation, Conceptualization. **Trust M. Pfukwa:** Writing – review & editing, Methodology. **Doctor M.N. Mthiyane:** Writing – review & editing, Supervision, Resources. **Olaniyi A. Fawole:** Writing – review & editing, Supervision, Resources. **Damian C. Onwudiwe:** Writing – review & editing, Supervision, Resources, Conceptualization.

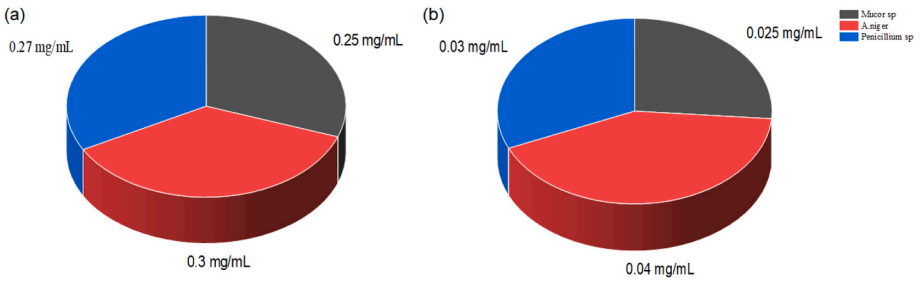

Fig. 7. Pie chart of the antifungal activity of (a) CuO and (b) Ce-doped CuO nanoparticles.

Table 5
Comparison of the antifungal activity of CuO and Ce-doped CuO nanoparticles with reported metal oxide nanoparticles in literature.

Nanoparticle	Innoculum density	Nanoparticle concentration	Fungal toxicity	Ref
CuO NPs	10^6	–	0.06 mg/mL	[49]
ZnOTiO2 NPs	10^8	–	0.625 mg/mL	[50]
Fe2O3	10^3	0.50 mg/mL	0.016	[51]
CuO	1-5 × 10^5	0.025–3.2 mg/mL	0.3 mg/mL	This study
Ce-doped CuO	1-5 × 10^5	0.025–3.2 mg/mL	0.04 mg/mL	This study

Declaration of competing interest

The authors have no relevant financial or non-financial interest to disclose.

Acknowledgement

The authors gratefully acknowledge the financial supports of the National Research Foundation of South Africa (Grant Number: SPAR231013155231), and North-West University (UID IK002799) for this research.

References

[1] L. Czaplewski, R. Bax, M. Clokie, M. Dawson, H. Fairhead, V.A. Fischetti, S. Foster, B.F. Gilmore, R.E. Hancock, D. Harper, I.R. Henderson, K. Hilpert, B.V. Jones, A. Kadioglu, D. Knowles, S. Olafsdottir, D. Payne, S. Projan, S. Shaunak, J. Silverman, C.M. Thomas, T.J. Trust, P. Warn, J.H. Rex, Alternatives to antibiotics-a pipeline portfolio review, Lancet Infect. Dis. 16 (2016) 239–251, https://doi.org/10.1016/S1473-3099(15)00466-1.
[2] I.D.S.o. America, Combating antimicrobial resistance: policy recommendations to save lives, Clin. Infect. Dis. 52 (2011) S397–S428.
[3] T.M. Belete, Novel targets to develop new antibacterial agents and novel alternatives to antibacterial agents, Human Microbiome Journal 11 (2019) 100052, https://doi.org/10.1016/j.humic.2019.01.001.
[4] S.K. Mondal, S. Chakraborty, S. Manna, S.M. Mandal, Antimicrobial nanoparticles: current landscape and future challenges, RSC Pharmaceutics 1 (2024) 388–402, https://doi.org/10.1039/d4pm00032c.
[5] H.F. Hetta, Y.N. Ramadan, A.I. Al-Harbi, E.A. Ahmed, B. Battah, N.H. Abd Ellah, S. Zanetti, M.G. Donadu, Nanotechnology as a promising approach to combat multidrug resistant bacteria: a comprehensive review and future perspectives, Biomedicines 11 (2) (2023) 413, https://doi.org/10.3390/biomedicines11020413.
[6] P. Ioannou, S. Baliou, G. Samonis, Nanotechnology in the diagnosis and treatment of antibiotic-resistant infections, Antibiotics 13 (2) (2024) 121, https://doi.org/10.3390/antibiotics13020121.
[7] N.Y. Lee, W.C. Ko, P.R. Hsueh, Nanoparticles in the treatment of infections caused by multidrug-resistant organisms, Front. Pharmacol. 10 (2019) 1153, https://doi.org/10.3389/fphar.2019.01153.
[8] H.A. Hemeg, Nanomaterials for alternative antibacterial therapy, Int. J. Nanomed. 12 (2017) 8211–8225, https://doi.org/10.2147/IJN.S132163.
[9] N. Beyth, Y. Houri-Haddad, A. Domb, W. Khan, R. Hazan, Alternative antimicrobial approach: nano-antimicrobial materials, Evid Based Complement Alternat Med 2015 (2015) 246012, https://doi.org/10.1155/2015/246012.
[10] A. Gupta, N.M. Saleh, R. Das, R.F. Landis, A. Bigdeli, K. Motamedchaboki, A. R. Campos, K. Pomeroy, M. Mahmoudi, V.M. Rotello, Synergistic antimicrobial therapy using nanoparticles and antibiotics for the treatment of multidrug-resistant bacterial infection, Nano Futures 1 (2017) 015004.
[11] Y. Zhao, X. Jiang, Multiple strategies to activate gold nanoparticles as antibiotics, Nanoscale 5 (2013) 8340–8350, https://doi.org/10.1039/c3nr01990j.
[12] J. Sawai, K. Himizu, O. Yamamoto, Kinetics of bacterial death by heated dolomite powder slurry, Soil Biol. Biochem. 37 (2005) 1484–1489.
[13] A. Thill, O. Zeyons, O. Spalla, F. Chauvat, J. Rose, M. Auffan, A.M. Flank, Cytotoxicity of CeO2 nanoparticles for Escherichia coli. Physico-chemical insight of the cytotoxicity mechanism, Environ. Sci. Technol. 40 (2006) 6151–6156, https://doi.org/10.1021/es060999b.
[14] I. Mohammed Sadiq, N. Chandrasekaran, A. Mukherjee, Studies on effect of TiO2 nanoparticles on growth and membrane permeability of Escherichia coli, Pseudomonas aeruginosa, and Bacillus subtilis, Curr. Nanosci. 6 (2010) 381–387.
[15] K. Giannousi, G. Sarafidis, S. Mourdikoudis, A. Pantazaki, C. Dendrinou-Samara, Selective synthesis of Cu(2)O and Cu/Cu(2)O NPs: antifungal activity to yeast Saccharomyces cerevisiae and DNA interaction, Inorg. Chem. 53 (2014) 9657–9666, https://doi.org/10.1021/ic501143z.
[16] N.V. Gandhare, R.G. Chaudhary, V.P. Meshram, J.A. Tanna, S. Lade, M. P. Gharpure, H.D. Juneja, An efficient and one-pot synthesis of 2, 4, 5-trisubstituted imidazole compounds catalyzed by copper nanoparticles, Journal of the Chinese Advanced Materials Society 3 (2015) 270–279.
[17] Y.H. Hsueh, P.H. Tsai, K.S. Lin, pH-dependent antimicrobial properties of copper oxide nanoparticles in Staphylococcus aureus, Int. J. Mol. Sci. 18 (2017) 793, https://doi.org/10.3390/ijms18040793.
[18] F. Nishino, M. Jeem, L. Zhang, K. Okamoto, S. Okabe, S. Watanabe, Formation of CuO nano-flowered surfaces via submerged photo-synthesis of crystallites and their antimicrobial activity, Sci. Rep. 7 (2017) 1063, https://doi.org/10.1038/s41598-017-01194-5.
[19] U. Bogdanovic, V. Vodnik, M. Mitric, S. Dimitrijevic, S.D. Skapin, V. Zunic, M. Budimir, M. Stoiljkovic, Nanomaterial with high antimicrobial efficacy–copper/polyaniline nanocomposite, ACS Appl. Mater. Interfaces 7 (2015) 1955–1966, https://doi.org/10.1021/am507746m.
[20] J. Zhou, H. Xiang, F. Zabihi, S. Yu, B. Sun, M. Zhu, Intriguing anti-superbug Cu 2 O@ ZrP hybrid nanosheet with enhanced antibacterial performance and weak cytotoxicity, Nano Res. 12 (2019) 1453–1460.
[21] E.M. Hotze, T. Phenrat, G.V. Lowry, Nanoparticle aggregation: challenges to understanding transport and reactivity in the environment, J. Environ. Qual. 39 (2010) 1909–1924, https://doi.org/10.2134/jeq2009.0462.
[22] M.S. Usman, M.E. El Zowalaty, K. Shameli, N. Zainuddin, M. Salama, N.A. Ibrahim, Synthesis, characterization, and antimicrobial properties of copper nanoparticles, Int. J. Nanomed. 8 (2013) 4467–4479, https://doi.org/10.2147/IJN.S50837.
[23] S.M. Morsy, Role of surfactants in nanotechnology and their applications, Int. J. Curr. Microbiol. App. Sci 3 (2014) 237–260.
[24] C.D. Venkatachalam, M. Sengottian, S.R. Ravichandran, Green synthesis of nanoparticles—metals and their oxides, in: R.P. Kumar, B. Bharathiraja (Eds.), Nanomaterials, Academic Press, 2021, pp. 79–96, https://doi.org/10.1016/b978-0-12-822401-4.00012-x.
[25] S. Ying, Z. Guan, P.C. Ofoegbu, P. Clubb, C. Rico, F. He, J. Hong, Green synthesis of nanoparticles: current developments and limitations, Environ. Technol. Innovat. 26 (2022) 102336, https://doi.org/10.1016/j.eti.2022.102336.
[26] N. Kataria, V.K. Garg, Green synthesis of Fe(3)O(4) nanoparticles loaded sawdust carbon for cadmium (II) removal from water: regeneration and mechanism, Chemosphere 208 (2018) 818–828, https://doi.org/10.1016/j.chemosphere.2018.06.022.
[27] S. Ashique Priya, O. Afzal, M. Khalid, M. Faruque Ahmad, A. Upadhyay, S. Kumar, A. Garg, M. Ramzan, A. Hussain, M.A. Altamimi, A.S.A. Altamimi, T.J. Webster, A. Khanam, Biogenic nanoparticles from waste fruit peels: synthesis, applications, challenges and future perspectives, Int. J. Pharm. 643 (2023) 123223, https://doi.org/10.1016/j.ijpharm.2023.123223.
[28] N. Munna, R. Abdur, R. Islam, M.S. Bashar, S.F.U. Farhad, M. Kamruzzaman, S. Aziz, M.A.A. Shaikh, M. Hossain, M.S. Jamal, Influence of Sn doping on the optoelectronic properties of ZnO nanoparticles, Nanoscale Adv. 5 (2023) 4996–5004, https://doi.org/10.1039/d3na00409k.
[29] A. Pinna, M. Torki Baghbaderani, V. Vigil Hernandez, P. Naruphontjirakul, S. Li, T. McFarlane, D. Hachim, M.M. Stevens, A.E. Porter, J.R. Jones, Nanoceria provides antioxidant and osteogenic properties to mesoporous silica nanoparticles for osteoporosis treatment, Acta Biomater. 122 (2021) 365–376, https://doi.org/10.1016/j.actbio.2020.12.029.

[30] S.M. Hirst, A.S. Karakoti, R.D. Tyler, N. Sriranganathan, S. Seal, C.M. Reilly, Anti-inflammatory properties of cerium oxide nanoparticles, Small 5 (2009) 2848–2856, https://doi.org/10.1002/smll.200901048.
[31] E.G. Heckert, A.S. Karakoti, S. Seal, W.T. Self, The role of cerium redox state in the SOD mimetic activity of nanoceria, Biomaterials 29 (2008) 2705–2709, https://doi.org/10.1016/j.biomaterials.2008.03.014.
[32] M.C. Ogwuegbu, A.S. Ayangbenro, D.M.N. Mthiyane, O.O. Babalola, D. C. Onwudiwe, Green synthesis of CuO nanoparticles using Ligustrum lucidum extract, and the antioxidant and antifungal evaluation, Mater. Res. Express 11 (2024) 055010, https://doi.org/10.1088/2053-1591/ad4e9d.
[33] C.K. Campbell, E.M. Johnson, Identification of Pathogenic Fungi, John Wiley & Sons, 2013.
[34] S.N. López, M.P. Sangorrín, M.B. Pildain, Fruit rot of sweet cherries and raspberries caused by Penicillium crustosum and Mucor piriformis in South Patagonia, Argentina, J. Indian Dent. Assoc. 38 (2016) 511–516.
[35] C. Valgas, S.M.d. Souza, E.F. Smânia, A. Smânia Jr., Screening methods to determine antibacterial activity of natural products, Braz. J. Microbiol. 38 (2007) 369–380.
[36] E.L. Berkow, S.R. Lockhart, L. Ostrosky-Zeichner, Antifungal susceptibility testing: current approaches, Clin. Microbiol. Rev. 33 (2020), https://doi.org/10.1128/CMR.00069-19.
[37] N. Zayyoun, L. Bahmad, L. Laânab, B. Jaber, The effect of pH on the synthesis of stable Cu 2 O/CuO nanoparticles by sol–gel method in a glycolic medium, Appl. Phys. A 122 (2016) 1–6.
[38] A. Barhoum, T. Favre, S. Sayegh, F. Tanos, E. Coy, I. Iatsunskyi, A. Razzouk, M. Cretin, M. Bechelany, 3D self-supported nitrogen-doped carbon nanofiber electrodes incorporated Co/CoOx nanoparticles: application to dyes degradation by electro-fenton-based process, Nanomaterials 11 (2021) 2686.
[39] T. Zhu, J. Yang, J. Liang, Z. Li, Y. Shen, Z. Yu, S. Wang, Y. Hou, Sn (IV)-doping induced higher lattice strain and activated more lattice oxygen in the Bi2O2CO3 for boosting photocatalytic activity: experimental and theoratical calculation study, Separ. Purif. Technol. 309 (2023) 122963, https://doi.org/10.1016/j.seppur.2022.122963.
[40] M. Farooq, S. Shujah, K. Tahir, S.T. Hussain, A.U. Khan, Z.M. Almarhoon, K. F. Alabbosh, A.A. Alanazi, T.M. Althagafi, M.E.A. Zaki, Phytoassisted synthesis of CuO and Ag-CuO nanocomposite, characterization, chemical sensing of ammonia, degradation of methylene blue, Sci. Rep. 14 (2024) 1618, https://doi.org/10.1038/s41598-024-51391-2.
[41] A.R. West, Solid State Chemistry and its Applications, John Wiley & Sons, 2022.
[42] M. Farahmandjou, M. Zarinkamar, T. Firoozabadi, Synthesis of Cerium Oxide (CeO2) nanoparticles using simple CO-precipitation method, Rev. Mexic. Fisica 62 (2016) 496–499.
[43] A. Muhammed, T.G. Asere, T.F. Diriba, Photocatalytic and antimicrobial properties of ZnO and Mg-doped ZnO nanoparticles synthesized using lupinus albus leaf extract, ACS Omega 9 (2024) 2480–2490, https://doi.org/10.1021/acsomega.3c07093.
[44] B. Abebe, E.A. Zereffa, A. Tadesse, H.C.A. Murthy, A review on enhancing the antibacterial activity of ZnO: mechanisms and microscopic investigation, Nanoscale Res. Lett. 15 (2020) 190, https://doi.org/10.1186/s11671-020-03418-6.
[45] S. Parveen, A.H. Wani, M.A. Shah, H.S. Devi, M.Y. Bhat, J.A. Koka, Preparation, characterization and antifungal activity of iron oxide nanoparticles, Microb. Pathog. 115 (2018) 287–292, https://doi.org/10.1016/j.micpath.2017.12.068.
[46] N. Thakur, Anu, K. Kumar, A. Kumar, Effect of (Ag, Zn) co-doping on structural, optical and bactericidal properties of CuO nanoparticles synthesized by a microwave-assisted method, Dalton Trans. 50 (2021) 6188–6203, https://doi.org/10.1039/D0DT04405A.
[47] R.M. Adnan, M. Mezher, A.M. Abdallah, R. Awad, M.I. Khalil, Synthesis, characterization, and antibacterial activity of Mg-doped CuO nanoparticles, Molecules 28 (1) (2023) 103, https://doi.org/10.3390/molecules28010103.
[48] F.J. Osonga, G. Eshun, S. Kalra, I. Yazgan, L. Sakhaee, R. Ontman, S. Jiang, O. A. Sadik, Influence of particle size and shapes on the antifungal activities of greener nanostructured copper against Penicillium italicum, ACS Agricultural Science & Technology 2 (2022) 42–56, https://doi.org/10.1021/acsagscitech.1c00102.
[49] M.M. Rahaman, Antifungal Activity of Copper Oxide (CuO) Nanoparticle (NP), vol. 2012, 2012, pp. 1–10.
[50] A. Irshad, R. Jawad, U. Ishtiaq, N. Joly, B. Bejaoui, N. M'Hamdi, P. Martin, F. Mubashar, Unveiling the power of TiO2 doped ZnO nanomaterial as an effective antimicrobial solution in the leather industry, Heliyon 10 (2024) e38414, https://doi.org/10.1016/j.heliyon.2024.e38414.
[51] S. Parveen, A.H. Wani, M.A. Shah, H.S. Devi, M.Y. Bhat, J.A. Koka, Preparation, characterization and antifungal activity of iron oxide nanoparticles, Microb. Pathog. 115 (2018) 287–292, https://doi.org/10.1016/j.micpath.2017.12.068.